The antiparasitic drug atovaquone inhibits arbovirus replication through the depletion of intracellular nucleotides.

Angelica Cifuentes Kottkamp[1], Elfie De Jesus[2], Rebecca Grande[2], Julia A. Brown[3,4], Adam R. Jacobs[5], Jean K. Lim[3], Kenneth A. Stapleford[2*]

[1]Department of Medicine, New York University School of Medicine, New York, NY, USA

[2]Department of Microbiology, New York University School of Medicine, New York, NY, USA

[3]Department of Microbiology, Icahn School of Medicine at Mount Sinai, New York, NY USA

[4]Graduate School of Biomedical Sciences, Icahn School of Medicine at Mount Sinai, New York, NY, USA

[5]Department of Obstetrics and Gynecology, Pediatrics, and Medical Education, Icahn School of Medicine at Mount Sinai, New York, NY, USA

* Corresponding author: Kenneth Stapleford. New York University School of Medicine, Department of Microbiology, New York, NY 10016. Kenneth.stapleford@nyumc.org

Short Title: Atovaquone inhibits arbovirus replication.

Abstract

Arthropod-borne viruses represent a significant public health threat worldwide yet there are few antiviral therapies or prophylaxis targeting these pathogens. In particular, the development of novel antivirals for high-risk populations such as pregnant women is essential to prevent devastating disease such as that which was experienced with the recent outbreak of Zika virus (ZIKV) in the Americas. One potential avenue to identify new and pregnancy friendly antiviral compounds is to repurpose well-known and widely used FDA approved drugs. In this study, we addressed the antiviral role of atovaquone, a FDA Pregnancy Category C drug and pyrimidine biosynthesis inhibitor used for the prevention and treatment of parasitic infections. We found that atovaquone was able to inhibit ZIKV and chikungunya virus virion production in human cells and that this antiviral effect occurred early during infection at the initial steps of viral RNA replication. Moreover, we were able to complement viral replication and virion production with the addition of exogenous pyrimidine nucleosides indicating that atovaquone is functioning through the inhibition of the pyrimidine biosynthesis pathway to inhibit viral replication. Finally, using an *ex vivo* human placental tissue model, we found that atovaquone could limit ZIKV infection in a dose-dependent manner providing evidence that atovaquone may function as an antiviral in humans. Taken together, these studies suggest that atovaquone could be a broad-spectrum antiviral drug and a potential attractive candidate for the prophylaxis or treatment of arbovirus infection in vulnerable populations, such as pregnant women.

Author Summary

The ability to protect vulnerable populations such as pregnant women and children from Zika virus and other arbovirus infections is essential to preventing the devastating complications induced by these viruses. One class of antiviral therapies may lie in known pregnancy-friendly drugs that have the potential to mitigate arbovirus infections and disease yet this has not been explored in detail. In this study, we show that the common antiparasitic drug, atovaquone, inhibits arbovirus replication through intracellular nucleotide depletion and can impair ZIKV infection in an *ex vivo* human placental explant model. Our study provides a novel function for atovaquone and highlights that the rediscovery of pregnancy-acceptable drugs with potential antiviral effects can be the key to better addressing the immediate need for treating viral infections and preventing potential birth complications and future disease.

Introduction

Recent outbreaks of significant human vector-borne pathogens have left us with the uncertainty of potential future devastating epidemics [1], [2]. In particular, Zika virus (ZIKV), a flavivirus and close relative of dengue virus (DENV), has led to an overwhelming spectrum of diseases, including Guillain-Barré syndrome, microcephaly, ocular and testicular damage, and even meningitis, encephalitis, thrombocytopenia and multiorgan failure [3], [4], [5], [6], [7], [8]. This, coupled with the widespread and invasive *Aedes* species of mosquito makes it easy to envision another epidemic when environmental, ecological, and human factors meet [9]. Unfortunately, there are no antiviral treatments or prophylaxes targeting these viruses, and thus efforts to mitigate and ultimately prevent the impact of the disease are urgent and need to be addressed.

Pregnant women carry a particularly high risk for ZIKV and other arbovirus-related complications [10], [11], [12]. Importantly, the capacity of the virus to infect trophoblasts, Hofbauer macrophages and endothelial cells [1], [13], thus allowing it to infect the fetus at any stage of growth, challenges the protective function of the placenta in the materno-fetal interface [14],[15]. Despite the significant morbidity observed in newborns [16], there are no antivirals available to treat this population in part due to safety concerns during pregnancy, lack of biosafety studies and nonexistent clinical trials. With this in mind, and given the urgency of this need, we propose to repurpose existing drugs with an acceptable profile in pregnancy.

Nucleotide biosynthesis inhibitors such as ribavirin, brequinar, and mycophenolic acid (MPA) have been shown extensively to inhibit a wide array of viral infections both *in vitro* and *in vivo* [17], [18], [19], [20], [21] [22], [23]. In addition, a number of small compounds that possess antiviral function through the depletion of intracellular nucleotide pools have been identified, suggesting that this cellular pathway may be a prime target for antiviral development [24], [25], [26], [27], [28]. Unfortunately, many of these compounds have numerous side effects and are not approved for

use in high risk populations such as pregnant women or children, thus the development of safe and pregnancy-acceptable nucleotide biosynthesis inhibitors would be ideal candidates as antivirals.

In these studies, we address the antiviral role of atovaquone, a FDA Pregnancy Category C and well-known antimalarial and antiparasitic drug that has been used repeatedly in the clinical setting for nearly two decades [29] [30], [31], [32]. Atovaquone is a ubiquinone (Coenzyme Q) analogue that functions through the inhibition of the mitochondrial cytochrome complex III [33, 34]. However, it has also been shown to inhibit dihydroorotate dehydrogenase (DHODH), an enzyme required for *de novo* pyrimidine synthesis, leading to specific depletion of intracellular nucleotide pools [33], [35], [36], [37]. Given these capacities, we hypothesized that atovaquone may function similarly to other known nucleotide biosynthesis inhibitors and may inhibit RNA virus replication.

Here, we show that atovaquone is able to inhibit ZIKV and chikungunya virus (CHIKV) replication and virion production in human cells, similar to what has been shown for other pyrimidine biosynthesis inhibitors. Moreover, we found this effect to occur early in infection, during the initial steps of viral RNA synthesis and that viral inhibition can be rescued with the addition of exogenous pyrimidines, indicating this drug is functioning through the blocking of DHODH and depletion of intracellular nucleotides. Finally, we show that atovaquone can inhibit ZIKV infection in an *ex vivo* human placental tissue model. Taken together, these studies identify atovaquone as a potential pregnancy acceptable antiviral compound. More importantly, they highlight the potential to repurpose available drugs in the hopes to one day translate these findings to novel and safe approaches, preventing arbovirus-related outcomes of vulnerable populations.

Results

Atovaquone inhibits arbovirus replication *in vitro*. Nucleotide biosynthesis inhibitors have been shown to have antiviral activity towards a wide range of RNA viruses both *in vitro* and *in vivo* [18], [21], [26], [38], [39], [40], suggesting that manipulating this pathway is a potential avenue for antiviral development. However, many of these compounds are not approved for use in high-risk populations such as pregnant women. Atovaquone is a well-tolerated antiparasitic [31] drug that has been used extensively for the treatment and prevention of *pneumocystis jirovecii* pneumonia (PCP), toxoplasmosis, babesiosis and malaria [29], [30], [32], [34], yet the antiviral role of atovaquone has not been addressed. To examine the antiviral activity of atovaquone, we pretreated Vero cells with increasing concentrations of atovaquone as well as ribavirin, MPA, and brequinar, known nucleotide biosynthesis inhibitors shown to have antiviral function (**Figure 1**). The cells were subsequently infected with either the Ugandan or Brazilian strains of Zika virus (ZIKV) and viral inhibition was assessed 72 hours post infection by immunostaining for the ZIKV envelope (E) protein. We found that all known nucleotide biosynthesis inhibitors were able to inhibit ZIKV replication although in a strain specific manner (**Figure 1A-C**). Importantly, we found that atovaquone exhibited similar antiviral activity over the concentrations tested and that this inhibition was again strain specific (**Figure 1D-F**). Taken together, these studies show that atovaquone inhibits ZIKV infection and spread, potentially through the depletion of intracellular nucleotide pools.

Atovaquone impairs ZIKV virion production in human cells. Given the inhibition of viral replication in Vero cells, we next addressed whether atovaquone was able to reduce the production of infectious ZIKV particles in mammalian cell types including human cells. For these and all subsequent studies, we chose to use the Ugandan strain of ZIKV due to its robust replication *in vitro* and its relative resistance to atovaquone compared to the Brazilian strain (**Figure 1**). We infected Vero, human 293T and human placental JEG3 cells with the Ugandan

143 strain of ZIKV in the presence of atovaquone or a DMSO control and quantified infectious virion
144 production by plaque assay. We found that atovaquone significantly impaired virion production in
145 all cell types tested although the peak of inhibition varied between cell type (**Figure 2A-C**).

146 One potential explanation for these results could be that atovaquone is toxic, and this
147 leads to reduced virus production. To address this, we first measured cell viability by a MTT cell
148 proliferation assay and found that atovaquone indeed had a dose-dependent reduction in cell
149 proliferation compared to the DMSO control (**Figure S1A**). However, atovaquone is a
150 mitochondrial cytochrome complex III inhibitor [33, 36, 44] and thus we hypothesized that the MTT
151 assay results we observed may be due to mitochondrial inhibition and are not directly indicative
152 of dying cells. To confirm this, we measured cell viability with Sytox Green, a dye that binds nucleic
153 acids when both the plasma and the nuclear membrane are permeabilized and thus represents
154 dying cells (**Figure S1B**). Using this assay, we found that high concentrations of atovaquone,
155 particularly in 293T cells, did lead to more cell death than the DMSO control; however, lower
156 concentration, that did show effects by the MTT assay, had minimal effects on cell viability.
157 Moreover, these results were confirmed in our data as although we observed a reduction in cell
158 growth by MTT assay we found that in Vero and 293T cells, virus production increased at higher
159 concentrations of atovaquone suggesting that the cells are still competent for virus production
160 under these conditions. Taken together, these results show that atovaquone is able to inhibit ZIKV
161 virion production in mammalian and human cell types.

162 To expand on these findings, we addressed if atovaquone could inhibit chikungunya virus
163 (CHIKV), an arbovirus transmitted by *Aedes* mosquitoes and capable of causing severe human
164 disease and significant outbreaks [45], [46], [47]. Importantly, CHIKV has been shown to be
165 inhibited by nucleotide biosynthesis inhibitors [22], [48], [49], and thus we hypothesized it would
166 be inhibited by atovaquone. We infected Vero cells with a CHIKV expressing a ZsGreen reporter
167 in the presence of increasing concentrations of atovaquone and quantified the number of ZsGreen

positive cells after treatment by microscopy. Similar to ZIKV, CHIKV replication was inhibited by atovaquone in a dose-dependent manner (**Figure 3A**). This inhibition in replication was further confirmed in Vero and 293T cells where we observed reductions in infectious CHIKV virions after treatment with atovaquone (**Figure 3B**). These results suggest that atovaquone can inhibit multiple arboviruses and has the potential to be used as a well-tolerated antiviral therapy.

Atovaquone inhibits ZIKV at early stages of infection. To explore which stage of viral life cycle atovaquone targets, we first addressed viral entry by treating cells with atovaquone or DMSO during virus entry, washing the cells extensively, and adding back complete media (**Figure 4A**, at entry). As a control, we added atovaquone during entry and added back media containing atovaquone after infection (**Figure 4A**, post entry). We found that when cells are treated during viral entry there is no change in production of viral particles compared to DMSO yet when added after entry atovaquone was able to inhibit ZIKV replication suggesting that atovaquone functions post entry. To investigate this further, we performed time-of-addition experiments to test which part of the intracellular viral life cycle is targeted by atovaquone. We infected 293T cells with ZIKV, added atovaquone or a DMSO control at different time-points during infection (**Figure 4B**) and quantified viral titers by plaque assay at 36 hours post-infection. We found that ZIKV virion production is most inhibited at early stages of infection (up to 4 hours post infection) and that this effect diminishes as the infection progresses, suggesting that atovaquone acts early during infection, potentially inhibiting RNA replication. Finally, to investigate the impact of atovaquone on ZIKV RNA replication, we analyzed ZIKV intracellular RNA at multiple time points post infection (**Figure 4C**). We found that where viral RNA levels were equal after infection (time 0), again confirming there is no effect of atovaquone on viral entry, there was a significant difference in viral RNA at 24 and 48 hours post infection indicating that atovaquone is acting to inhibit ZIKV RNA replication early during infection.

ZIKV RNA replication and virion production is rescued by the addition of exogenous nucleosides. Given the role of atovaquone in the inhibition of DHODH and similar viral inhibition curves to brequinar, another inhibitor of DHODH and pyrimidine biosynthesis (**Figure 1B**), we hypothesized that atovaquone may function through a similar pathway. To address this, we performed a rescue experiment where we infected cells with ZIKV in the presence of atovaquone or DMSO followed by media with atovaquone supplemented with 100 μM uridine, cytidine, adenosine, or guanosine. We found that in all cells types, ZIKV infectious particle production was rescued only when uridine was added to the media (**Figure 5A-C**). Given these results and the dual function of atovaquone in blocking both mitochondrial function and DHODH, it is possible that the addition of exogenous nucleosides could simply have rescued the MTT phenotype (mitochondrial function) we see for atovaquone and thus ZIKV replication. However, we found that when cells were incubated in the presence of atovaquone and nucleoside there was no change in MTT cell proliferation (**Figure S2**), indicating that the ZIKV inhibition and rescue we observe is not through mitochondrial inhibition but rather through the inhibition of DHODH. Furthermore, we addressed the ability of uridine to complement ZIKV RNA synthesis and found that indeed the addition of exogenous uridine rescued this phenotype to similar levels of the DMSO control (**Figure 5D**). Taken together, these results suggest that atovaquone is functioning through the depletion of intracellular nucleotide pools, and the addition of exogenous uridine can rescue ZIKV replication via the pyrimidine salvage pathway, bypassing the inhibition of atovaquone at critical steps in the *de novo* pyrimidine synthesis inhibition.

Atovaquone inhibits ZIKV infection in an *ex vivo* human placental tissue model. We found that atovaquone significantly inhibited ZIKV in human placental JEG3 cells *in vitro* and thus were interested in determining the extent to which this compound could inhibit ZIKV infection in an *ex vivo* human placental tissue model. To investigate this, we infected human placental chorionic villus explants with the Ugandan strain of ZIKV in the presence of increasing doses of atovaquone.

Similar to data in cell lines, we found that ZIKV infection and virion production were inhibited in a dose-dependent manner in the human placental tissue (**Figure 6A**). These results were confirmed by fluorescence *in situ* hybridization probing for ZIKV RNA in ZIKV infected tissue where atovaquone treatment reduced ZIKV spread (**Figure 6B**), showing a dose-dependent decrease in ZIKV-infected cells in the presence of increasing amounts of atovaquone. These data highlight that atovaquone may provide protection in the human placenta-fetal interface during ZIKV infection.

Discussion

It remains unknown when the next outbreak of ZIKV will occur, yet we know through past devastating epidemics, in which thousands of women and children were affected by this virus that we still have an urgent need for effective therapies against ZIKV infection [11], [50], [51]. Despite current potential protection from herd and self-immunity, environmental factors, and host-vector-virus interactions that keep ZIKV in the low incidence figures [1], [52], [53], [54], [55], preventing ZIKV and other arbovirus infections should be a priority. In recent years, many compounds have been proposed as potential anti-ZIKV agents following *in vitro* results [24], [25], [56], [57], [58], [59], [60], [61], [62], [63], [64], [65]. Some of these drugs have an extensive background in the medical field and offer attractive options, either alone or in combination, for treatment and perhaps prophylaxis of ZIKV infections; however, most of them remain inadequate to be used during pregnancy. Only chloroquine has been demonstrated in pregnancy animal models to be effective against ZIKV [56] [57] and none of them have been tested in humans in the context of ZIKV infection. Here, we propose a pregnancy-acceptable drug candidate for the treatment of ZIKV and other potential viral infections, highlighting the repurposing of FDA approved drugs as a possible avenue for antiviral development.

Atovaquone, a ubiquinone analogue approved in humans since 1999 for the treatment of *Pneumocystis jiroveci* pneumonia (PCP) [32], [34] and prevention of malaria [29], has no antiviral

activity described in the literature to date. However, given that atovaquone functions through the inhibition of pyrimidine biosynthesis, a pathway essential to viruses and the target of numerous antiviral compounds, we hypothesized that atovaquone may be antiviral as well. In this work, we addressed the antiviral role of atovaquone on ZIKV infections *in vitro* and in an *ex vivo* human placental tissue model, as well as explored the antiviral effect on CHIKV *in vitro*. We first screened atovaquone and the known nucleotide biosynthesis inhibitors and antiviral compounds, ribavirin, MPA, and brequinar, for their ability to inhibit two genetically distant strains of ZIKV. We found that ribavirin, MPA, and brequinar were able to inhibit ZIKV replication as has been shown previously and that atovaquone also led to inhibition of ZIKV replication behaving similarly to the pyrimidine biosynthesis inhibitor brequinar. Interestingly, we found that there was a strain-specific impact of the nucleotide biosynthesis inhibitors suggesting that genetic differences between the Ugandan and Brazilian strains may be responsible for the sensitivity to nucleotide depletion. Nonetheless, we concluded that atovaquone inhibits ZIKV replication similarly to other nucleotide biosynthesis inhibitors in Vero cells.

One potential caveat of these experiments could be that whereas we do detect reductions in ZIKV infected cells by immunofluorescence, this could have little impact on infectious virion production. To address this, we quantified infectious virus in the supernatant in the presence of atovaquone treatment compared to a DMSO control. As we saw with immunofluorescence, atovaquone was able to significantly reduce the amount of infectious virus in multiple mammalian cell types, including human placental cells over a subset of drug concentrations. Interestingly we found that in Vero and 293T cells, higher concentrations of drug had the least impact on virion production. One explanation for this could be that the virus has evolved to be resistant to atovaquone. However, we find this unlikely given the short time of infection and that drug resistance typically takes multiple passages. An additional explanation could be that at high concentrations, atovaquone is interfering with other cellular pathways that impede its antiviral

effects yet still results in the inhibition of mitochondrial function *in vitro*. This may be of particular importance for the use of atovaquone as an antiviral in humans. In the *in vitro* human cell culture system, the CC_{50} of atovaquone was roughly 10 μM which contrasts with historical trials of atovaquone taken orally at a doses of 750 mg every 6 hours for the treatment of toxoplasmosis, reporting steady serum concentrations in humans of roughly 50 μM without associated toxicity [36] [66] [67]. One possible explanation for this difference is that *in vitro* studies do not entirely represent all the biological interactions that take place in the human body. In addition, it is possible that at this high concentration, atovaquone is not antiviral and thus would need to be optimized at lower concentrations for its antiviral function in humans.

To address the stage in the viral life cycle where atovaquone acts, we performed viral entry assays by infecting cells in the presence or absence of atovaquone and then adding media with or without the compound after infection. Here, we found that adding atovaquone at the time of infection had no effect on virion production whereas adding atovaquone after infection was able to reduce ZIKV replication, indicating that atovaquone is acting post entry. We then performed time-of-addition assays where we added atovaquone one hour before, during, and at multiple time points post infection. We found that only early during infection, within the first two to four hours post infection, was atovaquone able to inhibit viral replication. These data are similar to what has been seen for the antiviral effects of brequinar on DENV [20], [41], suggesting atovaquone may function by a similar mechanism. Given these results, we hypothesized that atovaquone is functioning during the initial steps of ZIKV RNA replication and blocking virion production through the inhibition of RNA replication. When we quantified ZIKV RNA levels over time we found that indeed atovaquone treatment significantly reduced viral RNA synthesis.

Atovaquone is thought to function primarily through the inhibition of mitochondrial cytochrome complex III and thus inhibition of mitochondrial function in the parasite [34], [36], [37]. Using an MTT assay of cell proliferation measured through mitochondrial function we also saw

that atovaquone was able to reduce mitochondrial function in all cell lines we analyzed, yet these cells were shown to be viable by Sytox Green staining. Atovaquone also functions through inhibiting dihydroorotate dehydrogenase (DHODH) [33], an enzyme involved in pyrimidine biosynthesis and in particular the synthesis of uridine monophosphate (UMP). Given the striking similarities to brequinar, another pyrimidine biosynthesis inhibitor, and that atovaquone specifically inhibited ZIKV RNA synthesis we hypothesized that this inhibition was through intracellular nucleotide depletion. To address this, we added exogenous nucleosides in the presence of atovaquone and indeed found that the addition of uridine was able to rescue ZIKV infection in all cell types, although to various extents. Moreover, we found that the addition of uridine was able to specifically rescue ZIKV RNA synthesis indicating that the antiviral effects of the drugs are through the depletion of intracellular nucleotides. We found it interesting that human 293T and JEG3 cells were unable to be completely rescued with the addition of uridine. However, it has been shown that nucleotide depletion will induce an antiviral innate immune response [26], [27], [40], and we hypothesize that a similar mechanism may be induced in these cells allowing them to retain antiviral function in the presence of exogenous uridine. One striking finding was that atovaquone in the presence of cytidine had an additive antiviral effect in several cell lines suggesting again that multiple cellular pathways may be at play. Finally, we show that atovaquone also works to inhibit ZIKV infection in human first and second trimester placental explants. Many studies have shown that placental cytotrophoblasts, trophoblasts, syncytotrophoblasts, Hofbauer cells, and fibroblasts are susceptible to ZIKV [13], [15], [68], [69], [70], [71], [72]; thus recreating the dynamics of this infection and host-virus interaction at the placental level makes this study relevant to the most vulnerable target of ZIKV, pregnant women.

Taken together, we found that atovaquone, a pregnancy-acceptable and common antiparasitic drug, has antiviral activity against ZIKV and CHIKV which can be translated in the clinical setting into an attractive candidate for the treatment and prevention of arbovirus infections

in vulnerable populations as well as in individuals who live in or travel to endemic areas. Furthermore, patients with AIDS, chronic steroid users, and post-transplant patients that take atovaquone daily for the prevention of PCP, remain at high risk of acquiring multiple viral infections due to their impaired immune system. Therefore, it could be valuable to estimate the effect of atovaquone in viruses relevant to these patients such as human cytomegalovirus [73], herpes simplex virus [74], JC virus [75], and respiratory syncytial virus [76]. Atovaquone (in combination with proguanil hydrochloride) is already commercially available and broadly prescribed for malaria prophylaxis, yet so far there have not been proposed any clinical trials that address the relationship of atovaquone and ZIKV or CHIKV infections. This raises several questions: *i*) Are individuals who are/were taking atovaquone-proguanil (Malarone®) protected from viral threats as well? and *ii*) Does the broad administration of drugs which may unknowingly possess antiviral functions impact the evolution of viral infections? Future studies addressing these questions will be essential to understanding the antiviral function of atovaquone on viral evolution and disease. Nonetheless, these results contribute to the urgent need of finding effective ZIKV treatments especially for pregnant women, as these treatments should be readily accessible in order to ameliorate the teratogenic consequences of ZIKV across all trimesters of pregnancy. The studies completed here identified a potential candidate for these at-risk populations, yet more work is needed to define the complete antiviral role of atovaquone *in vivo.* Moreover, these studies have highlighted that repurposing drugs may provide fast avenues to the development of novel antiviral therapies and that we can potentially exploit FDA approved, pregnancy-friendly drugs to fight emerging viral threats.

Materials and Methods

Cells and viruses. Vero cells (CCL-81, ATCC) were cultured in Dulbecco Modified Eagle Medium (DMEM) (Corning) supplemented with 10% new born calf serum (NBCS, Gibco), 100 μg/mL penicillin-streptomycin (P/S) (Corning) at 37°C with 5% CO_2. BHK-21 (CCL-10, ATCC), 293T (CRL-3216, ATCC), and JEG3 (provided by Dr. Carolyn Coyne, University of Pittsburgh) were cultured in DMEM supplemented with 10% fetal bovine serum (FBS, Atlanta Biologicals), 1% nonessential amino acids (NEAA, Corning), and 1% P/S at 37°C with 5% CO_2. All cell lines were confirmed to be mycoplasma free.

The Ugandan (MR766) [77] and Brazilian (Paraiba_01/2015) [78] strains of ZIKV were generated from [79] infectious clones provided by Dr. Matthew Evans (Icahn School of Medicine at Mount Sinai) and Dr. Alexander Pletnev (National Institutes of Health), respectively. To generate initial viral stocks, each plasmid was transfected via lipofectamine 2000 reagent (Invitrogen) into 293T cells and virus containing supernatant was harvested 48 hours post transfection. A working viral stock was then generated by passaging the initial viral stock over Vero cells. Viral titers were quantified by plaque assay. In brief, 10-fold serial dilutions of each virus in DMEM were added to a confluent monolayer of Vero cells for 1 hour at 37°C. Following incubation, cells were overlaid with 0.8% agarose in DMEM and 2% NBCS and incubated at 37°C for five days. The cells were fixed with 4% formalin, agarose plugs were removed, and plaques were visualized by crystal violet.

Wild type CHIKV was generated from the La Reunion 06-049 infectious clone as previously described [79] [48]. A CHIKV La Reunion infectious clone expressing ZsGreen was constructed by standard molecular biology techniques. First, an AvrII restriction enzyme site was inserted 5' of the subgenomic promoter by site-directed mutagenesis using the primers (Forward 5' CACTAATCAGCTACACCTAGGATGGAGTTCATCCC 3' and Reverse 5' GGGATGAACTCCATCCTAGGTGTAGCTGATTAGTG 3'). The CHIKV subgenomic promoter

366 was then amplified by PCR (Forward 5' CCTAGGCCATGGCCACCTTTGCAAG 3' and Reverse
367 5' ACTAGTTGTAGCTGATTAGTGTTTAG 3') and subcloned into the AvrII site to generate a
368 CHIKV infectious clone containing two subgenomic promoters. Finally, the ZsGreen cassette was
369 amplified by PCR (Forward 5' GTGTACCTAGGATGGCCCAGTCCAAGCAC 3' and Reverse 5'
370 GCTATCCTAGGTTAACTAGTGGGCAAGGC 3') from a CHIKV infectious clone obtained from
371 Dr. Andres Merits (University of Tartu) and subcloned into the AvrII restriction enzyme site. The
372 complete cassette and subgenomic regions were sequenced to ensure there were no second-
373 site mutations. To generate infectious virus, each plasmid was linearized overnight with NotI,
374 phenol-chloroform extracted, ethanol precipitated, and used for *in vitro* transcription using the SP6
375 mMessage mMachine kit (Ambion). *In vitro* transcribed RNAs were phenol-chloroform extracted,
376 ethanol precipitated, aliquoted at 1 μg/μl, and stored at -80°C. 10 μg of each RNA was
377 electroporated into BHK-21 cells [23] and virus was harvested 48 hours post electroporation.
378 Working virus stocks were generated by passaging virus over BHK-21 cells and viral titers were
379 quantified by plaque assay as described above.

380 **Ethics Statement.** For these experimental studies, first and second trimester human placental
381 tissue was obtained within two hours of surgery from donors undergoing elective termination
382 under an IRB protocol approved by the Institutional Review Board for the Ichan School of Medicine
383 at Mt. Sinai (HS: 12-00145). All subjects provided informed written surgical consent for the use of
384 de-identified waste materials for educational research. Tissue specimens are considered to be
385 non-human subjects since they are de-identified. Following the surgery, tissue specimens are
386 delivered to Mount Sinai's Institutional Biorepository and Molecular Pathology Shared Resource
387 Facility (SRF) in the Department of Pathology. The biorepository operates under a Mount Sinai
388 Institutional Review Board (IRB) approved protocol and follows guidelines set by HIPAA. All
389 samples are linked, with appropriate IRB approval and consent, to clinical and pathological data,

and are open to all investigators of the institution, as well as to specific third-party collaborative efforts with investigators from other institutions.

***Ex vivo* infection of human placental tissue.** First and second trimester human placental tissue was obtained as described above. Chorionic villi adjacent to the fetal chorionic plate were placed into prewarmed DMEM containing 25% F-12 media, 10% FBS, 5 mM HEPES, 2 mM Glutamine, 100 IU/ml Penicillin, 100 μg/ml Streptomycin, 2.5 μg/ml Fungizone, and 300 ng/ml Timentin as previously described [80]. After removal of the amnion and decidua, the chorionic villi were cut into 0.2 cm^3 blocks; nine blocks were plated per well of a six-well plate onto collagen gelfoams (Cardinal Health) in 3 ml media, and 3 wells were used per condition (27 tissue blocks). Following an overnight incubation at 37°C, tissue blocks were individually infected with $1x10^5$ PFU $ZIKV^{MR766}$ in a volume of 5 μl that was pre-incubated with 15 μM, 5 μM, or 1.6 μM atovaquone for 1 hour. Atovaquone was maintained in the culture media at the same concentrations throughout 6 days of culture. Supernatants were collected and media changed every other day.

ZIKV plaque forming unit assay. ZIKV plaque forming units (PFU) were quantified on Vero cell monolayers whereby 250 μl of tissue culture supernatant was adsorbed for 2 hours at 37°C in 12 well plates, and cells were overlaid with 1.5 ml DMEM (Invitrogen) supplemented with 0.8% methyl cellulose, 2% FBS, and 50 μg/ml gentamicin sulfate. Cells were incubated for 5 days at 37°C, fixed with 4% paraformaldehyde, and stained with crystal violet for plaque visualization.

ZIKV RNA detection by *in situ* hybridization. Placental tissues from day 6 post infection were fixed in 10% neutral buffered formalin for 24 hours and placed back into PBS until paraffin embedding. *In situ* hybridization using RNAscope® was performed on 5 μm paraffin-embedded sections. Deparaffinization and target retrieval were performed using RNAscope® Universal Pretreatment Reagents (ACD #322380) following the manufacturer's protocol, and fluorescence *in situ* hybridization was subsequently performed according to the manufacturer's protocol (ACD# 323110) with RNAscope® Probe V-ZIKVsph2015 (ACD #467871) as previously described [56].

Following *in situ* hybridization, slides were mounted with Vectashield hard-set mounting medium with DAPI (Vector Laboratories) and analyzed using an AxioImager Z2 microscope (Zeiss) and Zen 2012 software (Zeiss).

Drug sensitivity assays. Vero cells (10,000 cells/well in a 96-well plate) were pretreated with media containing a carrier control or drug (ribavirin, mycophenolic acid, brequinar (Sigma) or atovaquone (ABCAM)) for 2 hours at 37°C. Following pre-incubation, cells were incubated with ZIKV or CHIKV-ZsGreen at a multiplicity of infection (MOI) of 0.1 in the presence of each drug or carrier control for 1 hour at 37°C. Cells were then washed extensively and media containing drug or carrier was added to each well. After incubation at 37°C for 48 h, cells were fixed with 4% paraformaldehyde and subject to immunostaining or visualized directly in the case of CHIKV-ZsGreen. In brief, following fixation the cells were washed with Perm-Wash buffer (BD Bioscience), permeabilized with 0.25% Triton-X 100 in phosphate buffered saline (PBS) (Gibco), and blocked with 0.2% bovine serum albumin (BSA) and 0.05% Saponin in PBS for 1 hour at room temperature (RT). Cells were then incubated with a monoclonal mouse antibody to the Flavivirus envelope protein (4G2) (Millipore) for 1 hr at RT. Following primary antibody incubation, cells were washed with Perm-Wash buffer and incubated with a secondary anti-mouse IgG antibody conjugated to Alexa488 for 1 hour at RT. DAPI staining protocol. Cells were then washed and infected cells were quantified on a CellInsight CX7 High-content microscope and screening platform using uninfected cells as a negative control and a cut-off for three standard deviations from negative to be scored as an infected cell.

To address the effect of atovaquone on infectious virion production, mammalian and insect cells were seeded as described above and infected with ZIKV at an MOI of 0.1 in the presence of increasing concentrations of atovaquone for 1 hr at 37°C. Cells were washed with PBS and incubated in media containing atovaquone or DMSO as a control for 36 hrs at 37°C. Virus containing supernatants were collected and viral titers were quantified by plaque assay.

Cell viability assays. Cell viability was measured using the CellTiter 96 non-radioactive cell proliferation assay (Promega), according to the manufacturer's protocol. Vero, 293T, and JEG3 cells (10,000 cells/well in a 96-well plate) were treated with increasing concentrations of atovaquone and incubated for 36 hours at 37°C. Following the incubation, 15 μL of dye solution was added to each well and incubated for 4 hours at 37°C with 5% CO2. The reaction was stopped by the addition of 100 μL of Solubilization/Stop Solution and the absorbance was measured at 570 nm in an EnVision microplate reader. The 50% cytotoxic concentration (CC_{50}) was calculated by a non-linear regression analysis of the dose-response curves. Cell viability was also assayed using Sytox Green (Invitrogen) following the manufacteurer's instructions. Sytox green positive cells were quantified on the CellInsight CX7 high-content microscope as described above.

RNA extractions and RT-qPCR. Intracellular viral RNA was extracted with TRIzol reagent (Invitrogen) following the manufacturer's instructions and used directly for cDNA synthesis with the Maxima H minus-strand kit (Thermo). Relative viral RNA levels were quantified using Power SYBR Green (Applied Biosystems) using the following primers [81]: GAPDH ((5'-GAAGGTCGGAGTCAACGGATTT -3' and 5'- GAATTTGCCATGGGTGGAAT -3') and ZIKV (5'-AGATGACTGCGTTGTGAAGC-3' and 5'- GAGCAGAACGGGACTTCTTC-3').

Virus entry and time-of-addition assays. To assay for the role of atovaquone in viral entry, 293T cells were infected with ZIKV at an MOI of 0.1 in the presence of 4.5 μM atovaquone for 1 hour at 37°C. Cells were washed extensively, complete media with or without 4.5 μM atovaquone was added back to the cells, and virus containing supernatants were collected 36 hours post infection. Viral titers were quantified by plaque assay. As a control, media containing atovaquone was added after infection.

For time-of-addition studies, 293T cells, pretreated with 4.5 μM atovaquone for 1 hour or left untreated, were infected with ZIKV at an MOI of 0.1 in the presence or absence of atovaquone

for 1h at 37°C. Following incubation, cells were washed to remove unabsorbed virus and media with or without atovaquone was added. At different time points post-infection, media was removed and media containing 4.5 μM atovaquone was added to the infected cells. Culture medium was collected at 36 hours post infection and viral titers were quantified by plaque assay. Media containing DMSO was used as a control for all time points.

Rescue assay. Vero, 293T, JEG3, and C6/36 cells were seeded in a 96-well plate as described above. Cells were infected with ZIKV diluted to an MOI of 0.1 in DMEM containing atovaquone for 1h at 37°C. Following incubation, cells were washed three times with PBS to remove unabsorbed virus. After wash, cells were incubated with media containing atovaquone with either DMSO, or 100 μM uridine, cytidine, adenosine, or guanosine for 36hrs. Culture medium was collected at 36 hours post infection and viral titers quantified by plaque assay.

Data analysis and statistics. GraphPad Prism 7.0 software was used for all analyses. The equations to fit the best curve were generated based on R2 values ≥ 0.9 [inhibitory concentration vs normalized response]. Two-way ANOVA and Students *t*-tests were also used, with P values <0.05 considered statistically significant.

ACKNOWLEDGMENTS

We thank all members of the Stapleford lab for support and helpful discussions during the course of the study. We thank Aaron Briley and Meike Dittmann for technical assistance with the CX7 CellInsight High content microscopy and helpful discussion. Finally, we thank the labs of Drs. Carolyn Coyne, Matthew Evans, and Alexander Pletnev for essential cells and reagents.

References

1. Pierson TC, Diamond MS. The emergence of Zika virus and its new clinical syndromes. Nature. 2018;560(7720):573-81.

2. Duffy MR, Chen TH, Hancock WT, Powers AM, Kool JL, Lanciotti RS, et al. Zika virus outbreak on Yap Island, Federated States of Micronesia. N Engl J Med. 2009;360(24):2536-43.

3. Swaminathan S, Schlaberg R, Lewis J, Hanson KE, Couturier MR. Fatal Zika Virus Infection with Secondary Nonsexual Transmission. N Engl J Med. 2016;375(19):1907-9.

4. Karimi O, Goorhuis A, Schinkel J, Codrington J, Vreden SGS, Vermaat JS, et al. Thrombocytopenia and subcutaneous bleedings in a patient with Zika virus infection. Lancet. 2016;387(10022):939-40.

5. Pradhan F, Burns JD, Agameya A, Patel A, Alfaqih M, Small JE, et al. Case Report: Zika Virus Meningoencephalitis and Myelitis and Associated Magnetic Resonance Imaging Findings. Am J Trop Med Hyg. 2017;97(2):340-3.

6. Carteaux G, Maquart M, Bedet A, Contou D, Brugieres P, Fourati S, et al. Zika Virus Associated with Meningoencephalitis. N Engl J Med. 2016;374(16):1595-6.

7. de Oliveira Dias JR, Ventura CV, de Paula Freitas B, Prazeres J, Ventura LO, Bravo-Filho V, et al. Zika and the Eye: Pieces of a Puzzle. Prog Retin Eye Res. 2018;66:85-106.

8. Dirlikov E, Torres JV, Martines RB, Reagan-Steiner S, Perez GV, Rivera A, et al. Postmortem Findings in Patient with Guillain-Barre Syndrome and Zika Virus Infection. Emerg Infect Dis. 2018;24(1):114-7.

9. Kraemer MU, Sinka ME, Duda KA, Mylne AQ, Shearer FM, Barker CM, et al. The global distribution of the arbovirus vectors Aedes aegypti and Ae. albopictus. Elife. 2015;4:e08347.

10. Oliveira Melo AS, Malinger G, Ximenes R, Szejnfeld PO, Alves Sampaio S, Bispo de Filippis AM. Zika virus intrauterine infection causes fetal brain abnormality and microcephaly: tip of the iceberg? Ultrasound Obstet Gynecol. 2016;47(1):6-7.

512 11. Honein MA. Recognizing the Global Impact of Zika Virus Infection during Pregnancy. N
513 Engl J Med. 2018;378(11):1055-6.
514 12. Marinho PS, Cunha AJ, Amim Junior J, Prata-Barbosa A. A review of selected Arboviruses
515 during pregnancy. Matern Health Neonatol Perinatol. 2017;3:17.
516 13. de Noronha L, Zanluca C, Burger M, Suzukawa AA, Azevedo M, Rebutini PZ, et al. Zika
517 Virus Infection at Different Pregnancy Stages: Anatomopathological Findings, Target Cells and
518 Viral Persistence in Placental Tissues. Front Microbiol. 2018;9:2266.
519 14. Sheridan MA, Yunusov D, Balaraman V, Alexenko AP, Yabe S, Verjovski-Almeida S, et
520 al. Vulnerability of primitive human placental trophoblast to Zika virus. Proc Natl Acad Sci U S A.
521 2017;114(9):E1587-E96.
522 15. Quicke KM, Bowen JR, Johnson EL, McDonald CE, Ma H, O'Neal JT, et al. Zika Virus
523 Infects Human Placental Macrophages. Cell Host Microbe. 2016;20(1):83-90.
524 16. Hussain A, Ali F, Latiwesh OB, Hussain S. A Comprehensive Review of the Manifestations
525 and Pathogenesis of Zika Virus in Neonates and Adults. Cureus. 2018;10(9):e3290.
526 17. Hinton TM, Zuwala K, Deffrasnes C, Todd S, Shi S, Marsh GA, et al. Polyanionic
527 Macromolecular Prodrugs of Ribavirin: Antiviral Agents with a Broad Spectrum of Activity. Adv
528 Healthc Mater. 2016;5(5):534-40.
529 18. Snell NJ. Ribavirin--current status of a broad spectrum antiviral agent. Expert Opin
530 Pharmacother. 2001;2(8):1317-24.
531 19. Kamiyama N, Soma R, Hidano S, Watanabe K, Umekita H, Fukuda C, et al. Ribavirin
532 inhibits Zika virus (ZIKV) replication in vitro and suppresses viremia in ZIKV-infected STAT1-
533 deficient mice. Antiviral Res. 2017;146:1-11.
534 20. Qing M, Zou G, Wang QY, Xu HY, Dong H, Yuan Z, et al. Characterization of dengue virus
535 resistance to brequinar in cell culture. Antimicrob Agents Chemother. 2010;54(9):3686-95.
536 21. Goebel S, Snyder B, Sellati T, Saeed M, Ptak R, Murray M, et al. A sensitive virus yield
537 assay for evaluation of Antivirals against Zika Virus. J Virol Methods. 2016;238:13-20.

538 22. Coffey LL, Beeharry Y, Borderia AV, Blanc H, Vignuzzi M. Arbovirus high fidelity variant
539 loses fitness in mosquitoes and mice. Proc Natl Acad Sci U S A. 2011;108(38):16038-43.
540 23. Rozen-Gagnon K, Stapleford KA, Mongelli V, Blanc H, Failloux AB, Saleh MC, et al.
541 Alphavirus mutator variants present host-specific defects and attenuation in mammalian and
542 insect models. PLoS Pathog. 2014;10(1):e1003877.
543 24. da Silva S, Oliveira Silva Martins D, Jardim ACG. A Review of the Ongoing Research on
544 Zika Virus Treatment. Viruses. 2018;10(5).
545 25. Saiz JC, Oya NJ, Blazquez AB, Escribano-Romero E, Martin-Acebes MA. Host-Directed
546 Antivirals: A Realistic Alternative to Fight Zika Virus. Viruses. 2018;10(9).
547 26. Lucas-Hourani M, Dauzonne D, Jorda P, Cousin G, Lupan A, Helynck O, et al. Inhibition
548 of pyrimidine biosynthesis pathway suppresses viral growth through innate immunity. PLoS
549 Pathog. 2013;9(10):e1003678.
550 27. Luthra P, Naidoo J, Pietzsch CA, De S, Khadka S, Anantpadma M, et al. Inhibiting
551 pyrimidine biosynthesis impairs Ebola virus replication through depletion of nucleoside pools and
552 activation of innate immune responses. Antiviral Res. 2018;158:288-302.
553 28. Raveh A, Delekta PC, Dobry CJ, Peng W, Schultz PJ, Blakely PK, et al. Discovery of
554 potent broad spectrum antivirals derived from marine actinobacteria. PLoS One.
555 2013;8(12):e82318.
556 29. Ling J, Baird JK, Fryauff DJ, Sismadi P, Bangs MJ, Lacy M, et al. Randomized, placebo-
557 controlled trial of atovaquone/proguanil for the prevention of Plasmodium falciparum or
558 Plasmodium vivax malaria among migrants to Papua, Indonesia. Clin Infect Dis. 2002;35(7):825-
559 33.
560 30. Krause PJ, Lepore T, Sikand VK, Gadbaw J, Jr., Burke G, Telford SR, 3rd, et al.
561 Atovaquone and azithromycin for the treatment of babesiosis. N Engl J Med. 2000;343(20):1454-
562 8.

563 31. Tan KR, Fairley JK, Wang M, Gutman JR. A survey on outcomes of accidental
564 atovaquone-proguanil exposure in pregnancy. Malar J. 2018;17(1):198.
565 32. Kovacs JA. Efficacy of atovaquone in treatment of toxoplasmosis in patients with AIDS.
566 The NIAID-Clinical Center Intramural AIDS Program. Lancet. 1992;340(8820):637-8.
567 33. Ashton TM, Fokas E, Kunz-Schughart LA, Folkes LK, Anbalagan S, Huether M, et al. The
568 anti-malarial atovaquone increases radiosensitivity by alleviating tumour hypoxia. Nat Commun.
569 2016;7:12308.
570 34. Artymowicz RJ, James VE. Atovaquone: a new antipneumocystis agent. Clin Pharm.
571 1993;12(8):563-70.
572 35. Yeo AE, Seymour KK, Rieckmann KH, Christopherson RI. Effects of dual combinations of
573 antifolates with atovaquone or dapsone on nucleotide levels in Plasmodium falciparum. Biochem
574 Pharmacol. 1997;53(7):943-50.
575 36. Baggish AL, Hill DR. Antiparasitic agent atovaquone. Antimicrob Agents Chemother.
576 2002;46(5):1163-73.
577 37. Cushion MT, Collins M, Hazra B, Kaneshiro ES. Effects of atovaquone and diospyrin-
578 based drugs on the cellular ATP of Pneumocystis carinii f. sp. carinii. Antimicrob Agents
579 Chemother. 2000;44(3):713-9.
580 38. Adcock RS, Chu YK, Golden JE, Chung DH. Evaluation of anti-Zika virus activities of
581 broad-spectrum antivirals and NIH clinical collection compounds using a cell-based, high-
582 throughput screen assay. Antiviral Res. 2017;138:47-56.
583 39. Tong X, Smith J, Bukreyeva N, Koma T, Manning JT, Kalkeri R, et al. Merimepodib, an
584 IMPDH inhibitor, suppresses replication of Zika virus and other emerging viral pathogens. Antiviral
585 Res. 2018;149:34-40.
586 40. Chung DH, Golden JE, Adcock RS, Schroeder CE, Chu YK, Sotsky JB, et al. Discovery
587 of a Broad-Spectrum Antiviral Compound That Inhibits Pyrimidine Biosynthesis and Establishes

588 a Type 1 Interferon-Independent Antiviral State. Antimicrob Agents Chemother. 2016;60(8):4552-
589 62.
590 41. Yeo KL, Chen YL, Xu HY, Dong H, Wang QY, Yokokawa F, et al. Synergistic suppression
591 of dengue virus replication using a combination of nucleoside analogs and nucleoside synthesis
592 inhibitors. Antimicrob Agents Chemother. 2015;59(4):2086-93.
593 42. Bassi MR, Sempere RN, Meyn P, Polacek C, Arias A. Extinction of Zika Virus and Usutu
594 Virus by Lethal Mutagenesis Reveals Different Patterns of Sensitivity to Three Mutagenic Drugs.
595 Antimicrob Agents Chemother. 2018;62(9).
596 43. Kim JA, Seong RK, Kumar M, Shin OS. Favipiravir and Ribavirin Inhibit Replication of
597 Asian and African Strains of Zika Virus in Different Cell Models. Viruses. 2018;10(2).
598 44. Siregar JE, Kurisu G, Kobayashi T, Matsuzaki M, Sakamoto K, Mi-ichi F, et al. Direct
599 evidence for the atovaquone action on the Plasmodium cytochrome bc1 complex. Parasitol Int.
600 2015;64(3):295-300.
601 45. Burt FJ, Chen W, Miner JJ, Lenschow DJ, Merits A, Schnettler E, et al. Chikungunya virus:
602 an update on the biology and pathogenesis of this emerging pathogen. Lancet Infect Dis.
603 2017;17(4):e107-e17.
604 46. Hua C, Combe B. Chikungunya Virus-Associated Disease. Curr Rheumatol Rep.
605 2017;19(11):69. Epub 2017/10/07. doi: 10.1007/s11926-017-0694-0. PubMed PMID: 28983760.
606 47. Vanlandingham DL, Higgs S, Huang YJ. Aedes albopictus (Diptera: Culicidae) and
607 Mosquito-Borne Viruses in the United States. J Med Entomol. 2016;53(5):1024-8.
608 48. Stapleford KA, Rozen-Gagnon K, Das PK, Saul S, Poirier EZ, Blanc H, et al. Viral
609 Polymerase-Helicase Complexes Regulate Replication Fidelity To Overcome Intracellular
610 Nucleotide Depletion. J Virol. 2015;89(22):11233-44.
611 49. Gallegos KM, Drusano GL, DZ DA, Brown AN. Chikungunya Virus: In Vitro Response to
612 Combination Therapy With Ribavirin and Interferon Alfa 2a. J Infect Dis. 2016;214(8):1192-7.

613 50. Santos B, Coelho FC, Armstrong M, Saraceni V, Lemos C. Zika: an ongoing threat to
614 women and infants. Cad Saude Publica. 2018;34(11):e00038218.
615 51. Fauci AS, Morens DM. Zika Virus in the Americas--Yet Another Arbovirus Threat. N Engl
616 J Med. 2016;374(7):601-4.
617 52. Liu Y, Liu J, Du S, Shan C, Nie K, Zhang R, et al. Evolutionary enhancement of Zika virus
618 infectivity in Aedes aegypti mosquitoes. Nature. 2017;545(7655):482-6.
619 53. O'Reilly KM, Lowe R, Edmunds WJ, Mayaud P, Kucharski A, Eggo RM, et al. Projecting
620 the end of the Zika virus epidemic in Latin America: a modelling analysis. BMC Med.
621 2018;16(1):180.
622 54. Rossi SL, Ebel GD, Shan C, Shi PY, Vasilakis N. Did Zika Virus Mutate to Cause Severe
623 Outbreaks? Trends Microbiol. 2018;26(10):877-85.
624 55. Sassetti M, Ze-Ze L, Franco J, Cunha JD, Gomes A, Tome A, et al. First case of confirmed
625 congenital Zika syndrome in continental Africa. Trans R Soc Trop Med Hyg. 2018;112(10):458-
626 62.
627 56. Cao B, Parnell LA, Diamond MS, Mysorekar IU. Inhibition of autophagy limits vertical
628 transmission of Zika virus in pregnant mice. J Exp Med. 2017;214(8):2303-13.
629 57. Shiryaev SA, Mesci P, Pinto A, Fernandes I, Sheets N, Shresta S, et al. Repurposing of
630 the anti-malaria drug chloroquine for Zika Virus treatment and prophylaxis. Sci Rep.
631 2017;7(1):15771.
632 58. Yang S, Xu M, Lee EM, Gorshkov K, Shiryaev SA, He S, et al. Emetine inhibits Zika and
633 Ebola virus infections through two molecular mechanisms: inhibiting viral replication and
634 decreasing viral entry. Cell Discov. 2018;4:31.
635 59. Retallack H, Di Lullo E, Arias C, Knopp KA, Laurie MT, Sandoval-Espinosa C, et al. Zika
636 virus cell tropism in the developing human brain and inhibition by azithromycin. Proc Natl Acad
637 Sci U S A. 2016;113(50):14408-13.

638 60. Sacramento CQ, de Melo GR, de Freitas CS, Rocha N, Hoelz LV, Miranda M, et al. The
639 clinically approved antiviral drug sofosbuvir inhibits Zika virus replication. Sci Rep. 2017;7:40920.
640 61. Han Y, Mesplede T, Xu H, Quan Y, Wainberg MA. The antimalarial drug amodiaquine
641 possesses anti-ZIKA virus activities. J Med Virol. 2018;90(5):796-802.
642 62. Cao RY, Xu YF, Zhang TH, Yang JJ, Yuan Y, Hao P, et al. Pediatric Drug Nitazoxanide:
643 A Potential Choice for Control of Zika. Open Forum Infect Dis. 2017;4(1):ofx009.
644 63. Li Z, Brecher M, Deng YQ, Zhang J, Sakamuru S, Liu B, et al. Existing drugs as broad-
645 spectrum and potent inhibitors for Zika virus by targeting NS2B-NS3 interaction. Cell Res.
646 2017;27(8):1046-64.
647 64. Xu M, Lee EM, Wen Z, Cheng Y, Huang WK, Qian X, et al. Identification of small-molecule
648 inhibitors of Zika virus infection and induced neural cell death via a drug repurposing screen. Nat
649 Med. 2016;22(10):1101-7.
650 65. Chan JF, Chik KK, Yuan S, Yip CC, Zhu Z, Tee KM, et al. Novel antiviral activity and
651 mechanism of bromocriptine as a Zika virus NS2B-NS3 protease inhibitor. Antiviral Res.
652 2017;141:29-37.
653 66. Basco LK, Ramiliarisoa O, Le Bras J. In vitro activity of atovaquone against the African
654 isolates and clones of Plasmodium falciparum. Am J Trop Med Hyg. 1995;53(4):388-91.
655 67. Shanks GD, Gordon DM, Klotz FW, Aleman GM, Oloo AJ, Sadie D, et al. Efficacy and
656 safety of atovaquone/proguanil as suppressive prophylaxis for Plasmodium falciparum malaria.
657 Clin Infect Dis. 1998;27(3):494-9.
658 68. Szaba FM, Tighe M, Kummer LW, Lanzer KG, Ward JM, Lanthier P, et al. Zika virus
659 infection in immunocompetent pregnant mice causes fetal damage and placental pathology in the
660 absence of fetal infection. PLoS Pathog. 2018;14(4):e1006994. E
661 69. Miner JJ, Cao B, Govero J, Smith AM, Fernandez E, Cabrera OH, et al. Zika Virus Infection
662 during Pregnancy in Mice Causes Placental Damage and Fetal Demise. Cell. 2016;165(5):1081-
663 91.

664 70. Ribeiro MR, Moreli JB, Marques RE, Papa MP, Meuren LM, Rahal P, et al. Zika-virus-
665 infected human full-term placental explants display pro-inflammatory responses and undergo
666 apoptosis. Arch Virol. 2018.
667 71. Vermillion MS, Lei J, Shabi Y, Baxter VK, Crilly NP, McLane M, et al. Intrauterine Zika
668 virus infection of pregnant immunocompetent mice models transplacental transmission and
669 adverse perinatal outcomes. Nat Commun. 2017;8:14575.
670 72. Tabata T, Petitt M, Puerta-Guardo H, Michlmayr D, Wang C, Fang-Hoover J, et al. Zika
671 Virus Targets Different Primary Human Placental Cells, Suggesting Two Routes for Vertical
672 Transmission. Cell Host Microbe. 2016;20(2):155-66.
673 73. de la Camara R. CMV in Hematopoietic Stem Cell Transplantation. Mediterr J Hematol
674 Infect Dis. 2016;8(1):e2016031.
675 74. Munawwar A, Singh S. Human Herpesviruses as Copathogens of HIV Infection, Their
676 Role in HIV Transmission, and Disease Progression. J Lab Physicians. 2016;8(1):5-18.
677 75. Beltrami S, Gordon J. Immune surveillance and response to JC virus infection and PML.
678 J Neurovirol. 2014;20(2):137-49.
679 76. Waghmare A, Campbell AP, Xie H, Seo S, Kuypers J, Leisenring W, et al. Respiratory
680 syncytial virus lower respiratory disease in hematopoietic cell transplant recipients: viral RNA
681 detection in blood, antiviral treatment, and clinical outcomes. Clin Infect Dis. 2013;57(12):1731-
682 41.
683 77. Schwarz MC, Sourisseau M, Espino MM, Gray ES, Chambers MT, Tortorella D, et al.
684 Rescue of the 1947 Zika Virus Prototype Strain with a Cytomegalovirus Promoter-Driven cDNA
685 Clone. mSphere. 2016;1(5).
686 78. Tsetsarkin KA, Kenney H, Chen R, Liu G, Manukyan H, Whitehead SS, et al. A Full-Length
687 Infectious cDNA Clone of Zika Virus from the 2015 Epidemic in Brazil as a Genetic Platform for
688 Studies of Virus-Host Interactions and Vaccine Development. MBio. 2016;7(4).

689 79. Coffey LL, Vignuzzi M. Host alternation of chikungunya virus increases fitness while
690 restricting population diversity and adaptability to novel selective pressures. J Virol.
691 2011;85(2):1025-35.
692 80. Weisblum Y, Oiknine-Djian E, Vorontsov OM, Haimov-Kochman R, Zakay-Rones Z, Meir
693 K, et al. Zika Virus Infects Early- and Midgestation Human Maternal Decidual Tissues, Inducing
694 Distinct Innate Tissue Responses in the Maternal-Fetal Interface. J Virol. 2017;91(4).
695 81. Bayer A, Lennemann NJ, Ouyang Y, Bramley JC, Morosky S, Marques ET, Jr., et al. Type
696 III Interferons Produced by Human Placental Trophoblasts Confer Protection against Zika Virus
697 Infection. Cell Host Microbe. 2016;19(5):705-12.

698

699

700

701

702

703

704

705

706

707

708

709

710

Figure Legends

Figure 1: Nucleotide biosynthesis inhibitors impair ZIKV replication.

Vero cells were pretreated with (**A**) ribavirin, (**B**) brequinar, (**C**) mycophenolic acid, (**D**) atovaquone or carrier controls for two hours and subsequently infected with either the Ugandan (MR766) or Brazilian (Paraiba_01/2015) strain of ZIKV at a MOI of 0.1. Cells were fixed 72 hours post infection, stained with anti-flavivirus E antibody, and infected cells were quantified on a CellInsight CX7 high-content microscope. Data are represented as percent ZIKV positive cells compared to the carrier control. (**E and F**) Representative images of Ugandan **(E)** and Brazilian **(F)** atovaquone inhibition at 1.125 μM.

Figure 2: Atovaquone inhibits ZIKV infectious virion production in mammalian cells.

(**A**) Vero, (**B**) 293T, and (**C**) JEG3 cells were infected with ZIKV MR766 at an MOI of 0.1 in the presence of atovaquone (open symbols) or DMSO control (closed symbols). Virus containing supernatants were collected 36 hours post infection and infectious virus was quantified by plaque assay on Vero cells. The mean and SEM are shown, n=9, Students *t*-test, * $p<0.05$.

Figure 3: Atovaquone inhibits chikungunya virus replication.

(**A**). Vero cells were pretreated with DMSO or atovaquone (ATQ) for two hours and subsequently infected with CHIKV (IOL) expressing ZsGreen at a MOI of 0.1. After infection, virus was removed, cells washed and media containing atovaquone was added for 24 hours. Cells were then fixed and ZsGreen positive cells were quantified by a CellInsight CX7 high-content microscope. Data are represented as percent ZsGreen positive compared to the DMSO control. (**B**). 293T and Vero cells were infected with CHIKV ZsGreen at a MOI of 0.1 in the presence of 4.5 μM atovaquone. Unabsorbed virus was washed off and media was added containing DMSO or 4.5 μM atovaquone. Infectious virus was quantified 24 hours post infection by plaque assay. The mean and SEM are shown, n=3, Students *t*-test. *** $p<0.005$.

Figure 4: Atovaquone acts early during ZIKV infection and inhibits viral RNA synthesis.

(**A**). 293T cells were infected with ZIKV MR766 at an MOI of 0.5 in the presence of 4.5 μM atovaquone. After absorption, cells were washed extensively, and media was added without (at entry) or with (post entry) 4.5 μM atovaquone. Infection virus was quantified by plaque assay 36 hours post infection. The mean and SEM are shown, n=4, Students *t*-test, * $p<0.05$. (**B**). 293T cells were treated with 4.5 μM atovaquone one hour prior, during, or post infection with ZIKV MR766 at a MOI of 1. After infection, virus was removed and media containing 4.5 μM atovaquone was added for 36 hours. Infectious virus was quantified by plaque assay 36 hours post infection. The mean and SEM are shown, n=3, Students *t*-test, * $p<0.05$, ** $p<0.01$ (**C**). Vero cells were infected with ZIKV MR766 at a MOI of 1 in the presence of 4.5 μM atovaquone. After infection, virus was removed, cells washed extensively, and media was added containing 4.5 μM atovaquone. At time 0 (after infection), 24, and 48 hours post infection, media was removed, cells washed, and intracellular RNA extracted with Trizol. Viral RNA was quantified by SYBR Green compared to GAPDH. The mean and SEM are shown, n=3, Students *t*-test, **** $p<0.0001$.

Figure 5: Exogenous uridine rescues ZIKV virion production and RNA synthesis.

(**A**) 293T, (**B**) JEG3, and (**C**) Vero cells were infected with ZIKV MR766 at a MOI of 0.1 in the presence of DMSO, atovaquone (293T and Vero = 4.5 μM atovaquone and JEG3 = 18 μM atovaquone), or atovaquone with 100 μM of uridine (U), cytidine (C), adenosine (A), or guanosine (G). After infection virus was removed, cells washed, and media was added containing DMSO, atovaquone, or atovaquone with 100 μM nucleoside. Infectious virus was quantified 36 hours post infection by plaque assay. The mean and SEM are shown, n=3, two-way ANOVA, * $p<0.05$, *** $p<0.005$, **** $p<0.0001$. (**D**). Vero cells were infected with ZIKV MR766 at a MOI of 1 in the presence of DMSO, 4.5 μM atovaquone, or 4.5 μM atovaquone with 100 μM uridine. Intracellular viral RNA was extracted with Trizol at 0, 24, and 48 hours post infection and viral RNA relative to

759 GAPDH was quantified by Sybr Green. The mean and SEM are shown, n=3, two-way ANOVA,
760 **** p<0.0001.

761 **Figure 6: Atovaquone inhibits ZIKV infection and spread in an *ex vivo* human placental**
762 **tissue model.** Human placental chorionic villus explants were infected with 10^5 PFU ZIKA
763 (MR766) in the presence of increasing concentrations of atovaquone or a DMSO carrier control.
764 Supernatants were collected at days 2, 4, and 6 post infection and viral titers were quantified by
765 plaque assay. **(A)** Total virus accumulation over the course of infection. The mean and SEM are
766 shown, n=3, two-way ANOVA, *** p<0.005. **(B)** Fluorescence *in situ* hybridization of ZIKV RNA
767 (red) infected human tissues counterstained with DAPI at 6 days post infection.

768

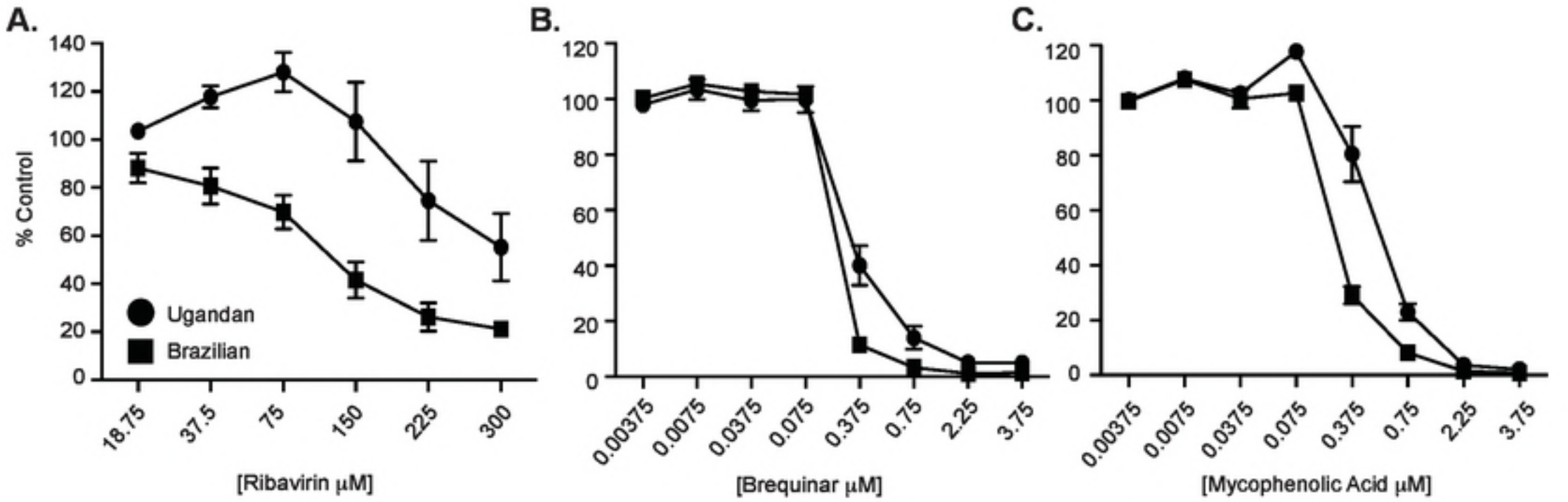

Figure 1 Kottkamp et al.

Figure